Texture Discrimination Analysis between Tumour and Healthy Brain Tissue Using MaZda Program

A.Z. Saleh[*] and R. A. Lerski[**]

[*]Department of Medical Physics, College of Medicine, University of Baghdad, Visitor at the Department of Medical Physics, Ninewells Hospital and Medical School-University of Dundee.
[**]Director of the Department of Medical Physics, Ninewells Hospital and Medical School-University of Dundee.

Abstract

Four MRI images were taken from patients with proven brain tumour. Images were analysed for texture discrimination using the MaZda program. The aim of the analysis was to discriminate between the tumour tissue and the healthy tissue counterpart for each patient. Three regions of interest were taken for the tumour and another three were taken for healthy tissue. Results of these analyses have shown a significant difference between the two tissues, it has given Fisher coefficients between (138.5 and 547.5) and very low p value much lower than 0.01. It is thought to be that the effect may be mainly attributed to the possible necrotic tissue as well as the bulk of cells in the tumour which may have altered the blood perfusion influencing the MR signal.

Keywords: texture analysis, tumour discrimination, brain tumour, MaZda program.

Introduction

There is an increasing importance of image texture analysis in the field of medical diagnostic radiology in attempt to improve the diagnostic facilities and explore hidden features in the images. An explanation for texture perception was presented by the psychologist (Gibson) at the beginning of the 1950s (1). After the development of computers a new texture approach has been introduced by using computer programs for analysis. The study of image texture in medical diagnosis was started in the early 1970s (2). A digital image is formed from pixels which are sufficiently small not to be recognised by the human eye. Analysis of such small entities may be considered as micro texture and may be defined as the study of gray level distribution characteristics. However much research work has been carried out in order to analyse and quantify texture in an attempt to improve medical diagnosis (3, 4, 5, 6, 7). Although there is no precise definition for texture, it is some times defined by the possession one or more property of fineness, coarseness, smoothness, granulation, randomness, lineation, mottled, irregularity (8, 9, 10, 11). For image texture analysis, several statistical methods have been designed for this purpose, such as the histogram and the co-occurrence matrix (12, 13, 14), wavelet transform (15, 16). Gradient matrix (13), Auto regressive model (9-17). The analyses of the image texture can be performed with the Mazda program (10, 11, 18). It analyses 275 features, these are -9- based on image histogram, -11- based on co occurrence matrix, this is calculated for four directions and -5- inter pixel distances (making 220 parameters), -5- run length matrix in -4- directions (make them 20), -5- gradient matrix, -5- first order autoregressive model, and -16- based on Harr wavelet transform calculated for -4- image scale factor (11).

Although the medical image texture may be not visible, in digital image where the gray level represented by numbers arranged in a matrix, texture can be detected and analysed by computer.

A tumour is an abnormal growth of cells and may contain necrotic region as well as the possible formation of oedema. Tumour cells are similar to the healthy cells forming the tumour tissue which is mainly different from healthy tissue in mass because it is packed with tumour cells making the tumour tissue denser. This difference between the healthy and tumour tissue is the main factor what the conventional x-ray and CT scanners modalities discriminating between the two tissues by differential absorption. A MRI signal is emitted from the unpaired protons in the atoms

forming the molecules so changes in the type or the abundance of an effective molecules can give a change in signal and if it is strong enough it will make a change in the gray level and have an effect on the image, this effect may not be recognised by eye depends on the value of the change in the gray level but it can be computer analysed. This is an important difference between the origin of MRI and x-ray and CT images, even with the ultrasound images which depends on the reflected acoustic wave according to the difference in the acoustic impedance.

In this work we have analysed tumours in MRI brain images the analysis was carried out by using Mazda program. The analysis involved four brain tumours which have been analysed with respect to the healthy brain tissue.

Method

Four patients (A, B, C, D) as shown in Fig. (1) were selected with proven brain tumours. Images were taken using Siemens MRI imager of 1.5T, they were loaded on MaZda program separately. Three regions of interest were chosen within the tumour and another three regions were chosen within the healthy region counterpart for the same patient. Then a texture analysis for comparison between the two regions was carried out.

Images were analysed in two classes (three ROI for the tumour in one class and another three ROI for healthy tissue as control in another class). The analyses Results were selected by using fisher coefficient (19), in which the best ten feature discrimination were selected. The selected data were introduced into B11 program for further selection and data reduction in addition to the availability of different analysis choices (10, 11). Then the desired discrimination analysis (raw data analysis) was performed.

Although the selection was performed in efficient statistical way we have also performed t-test examination to test the p value for the discriminated dataset

Results

Images were analysed by MaZda program. The analysis option was selected for all types of analysis in the program.
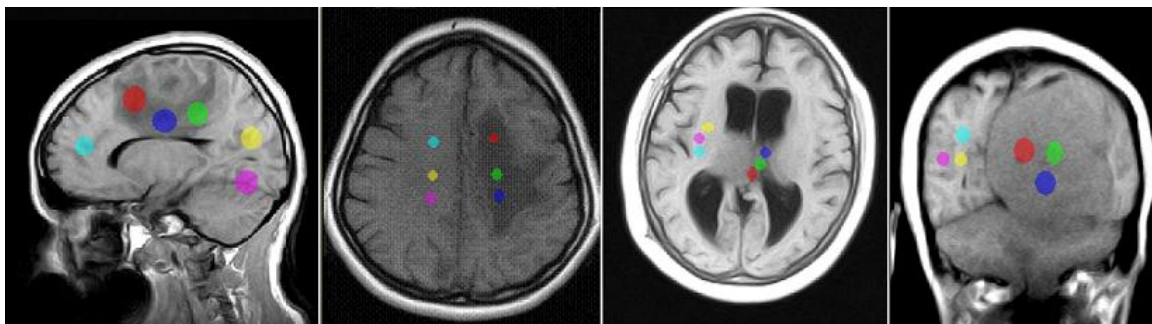
Fig.(1) Four MRI images with Brain tumour taken from four different patients for analysis.

Results show a clear discrimination between the tumour region and the healthy brain tissue with features selected using Fisher coefficient, which is the analysis of variance in between the class to the variance within the class. In fisher selection only the most ten significant features discrimination will be selected. Then data were further reduced in B11 program also provides the choice of analysis. Raw data analysis for the four images gave high fisher coefficients (218, 243.1, 547.8 and 138.5) for patients (A, B, C and D) respectively the (1-NN) 1-nearest neighbour misclassified 0/6 or 0%, Fig.(2, 3, 4, 5).

We have taken the first highest five features discrimination from the ten features chosen by fisher coefficient in sequence starting with the best feature discrimination, this is to find the p value. Results have shown highly significant discrimination between the tumour and healthy tissue, as has given p value much lower than (0.05) Tables (1, 2, 3, 4). The (*sumaverag)* feature was chosen for comparison because it is common between patients (B, C, D) it has given a high similarity in the discrimination between the tumour and healthy tissue Table (5).

Table (1)
The first five features taken from the ten features selected by fisher coefficient for patient A.

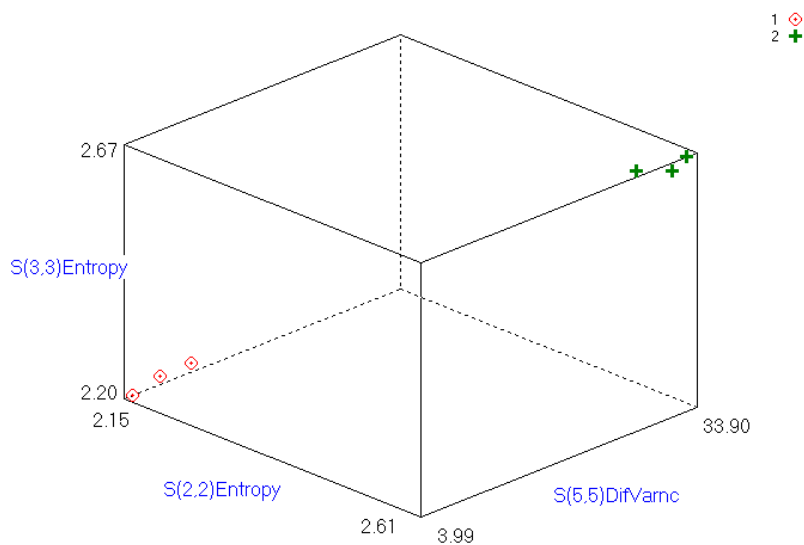| Patient A					
Tumour ROI	**Features (discrimination in sequence)**				
	S(5,5) Difentrop	**S(2,2) Entropy**	**S(3,3) Entropy**	**S(1,1) Entropy**	**S(4,4) DifVarnc**
1	0.9181	2.184	2.2	1.969	4.378
2	0.8722	2.203	2.268	2.019	3.603
3	0.9783	2.194	2.26	2.006	6.486
Normal ROI					
1	1.327	2.572	2.619	2.424	25.916
2	1.301	2.612	2.671	2.445	28.248
3	1.267	2.548	2.622	2.362	22.549
p-value	0.001403818	0.001171437	0.00018743	0.000469104	0.001531841

Fig.(2) Raw data discrimination analysis for patient (A) Fisher coefficient = 218 and 1-NN misclassified 0/6. Data labelled 1 and 2 represent the tumour and healthy tissue respectively.

<div align="center">

Table (2)
The first five features taken from the ten features selected by fisher coefficient for patient (B).

</div>

Tumour ROI	Features (discrimination in sequence)				
	Percentile 90%	*s(5,0) sumaverg*	*S(4,0) sumaverg*	*S(3,0) sumaverg*	*Percentile 99%*
1	64	125.5	124.12	122.75	65
2	68	128.5	129.3	129.81	71
3	69	135.8	135.3	134.65	71
Normal ROI					
1	106	201.17	203.27	203.62	107
2	104	200.5	200.8	199.62	105
3	101	193.33	194	194.27	103
p-value	6.53014E-05	8.54504E-05	9.47453E-05	0.000130258	0.00039798

(Patient B — header spanning the full table above the Tumour ROI section)
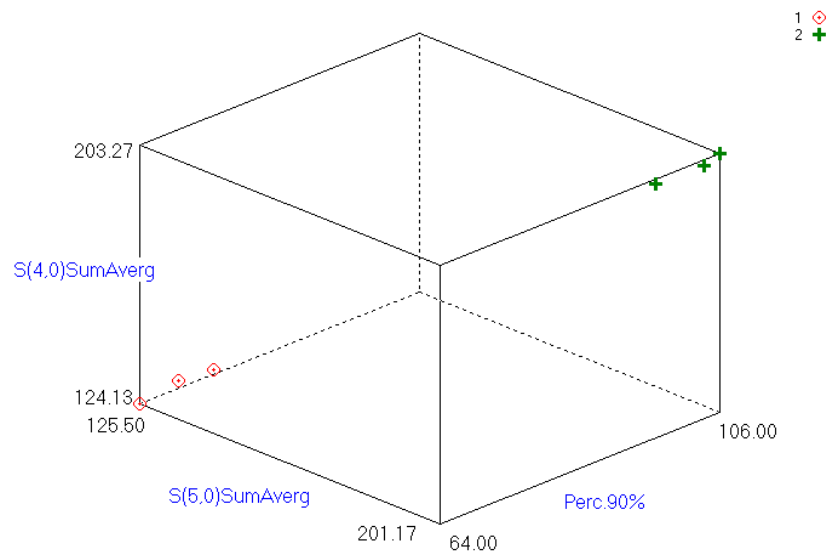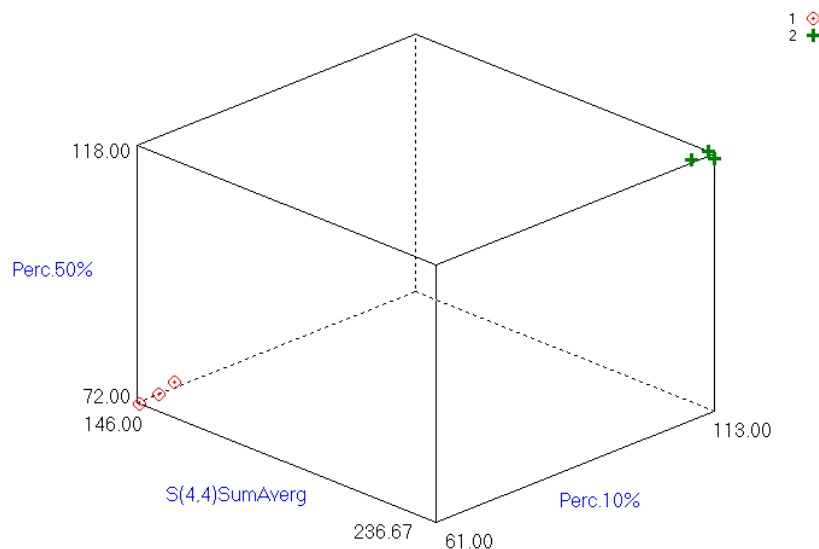

<div align="center">

Fig. (3) Raw data discrimination analysis for patient (B) Fisher coefficient = 243.1,
1-NN misclassified 0/6. Data labelled 1 and 2 represent the tumour and healthy
tissue respectively.

</div>

Table (3)
*The first five features taken from the ten features selected by fisher coefficient for patient C.*

Patient (C)					
Tumour ROI	**Features (discrimination in sequence)**				
	Percentile 10%	**S(4,4) sumaverg**	**Percentile 50%**	**S(0,5) sumaverg**	**S(4,4) sumaverg**
1	65	146	72	143.75	146.25
2	61	146.67	72	138.7	135.67
3	64	152.33	76	149.33	143.67
Normal ROI					
1	113	236.67	117	232.78	234.67
2	113	235	118	234	231.67
3	112	231.25	116	228.25	227
p-value	0.000256742	7.51437E-06	0.00227959	9.59198E-05	5.11022E-05

Fig.(4) Raw data discrimination analysis for patient (C) fisher number 547.8 and misclassified data vector 0/6. Data labelled 1 and 2 represent the tumour and healthy tissue respectively.

Table (4)
The first five features taken from the ten features selected by fisher coefficient for patient (D).

			Features (discrimination in sequence)		
	Patient (D)				
Tumour ROI	S(4,4) sumaverg	S(5,5) sumaverg	S(3,3) sumaverg	S(5,-5) sumaverg	S(4,-4) sumaverg
1	142.67	142.57	142.68	142.58	142.47
2	145.97	145.8	146.03	145.52	145.87
3	134.92	135.04	134.78	134.56	134.71
Normal ROI					
1	217.47	217.61	217.38	217.3	217.4
2	201.74	201.59	201.38	201.18	201.27
3	207.54	207.02	207.64	207.06	207.07
p-value	0.000482097	0.000576853	0.00050439	0.000552456	0.000550874
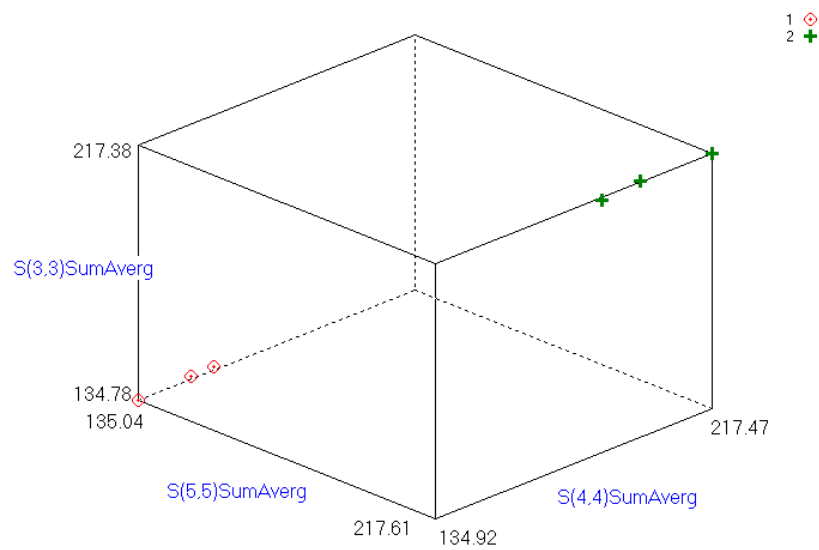
Fig.(5) Raw data discrimination analysis for patient (D) fisher number 138.5 and misclassified data vector 0/6. Data labelled 1 and 2 represent the tumour and healthy tissue respectively.

Table (5)
A sample of similar features taken from tables (2, 3, 4) for tumour and healthy tissues. A clear discrimination between the two tissues can be observed.

		Patient B	*Patient C*	*Patient D*		
		s(5,0) sumaverg	*S(4,4) sumaverg*	*S(5,5) sumaverg*		
Analysis for tumour ROI taken from 3 patients	ROI No.					AV
	1	125.5	146	142.57	AV	138.0233
	2	128.5	146.67	145.8	AV	140.3233
	3	135.8	152.33	135.04	AV	141.0567
						139.8011
SD		± 5.297483679	± 3.477388867	± 5.521343436	SD	± 1.582661
						AV
Analysis for healthy tissue ROI taken from 3 normals	1	201.17	236.67	217.61	AV	218.4833
	2	200.5	235	201.59	AV	212.3633
	3	193.33	231.25	207.02	AV	210.5333
						213.7933
SD		± 4.34594447	± 2.775722128	± 1.110314866	SD	± 4.163448

Discussion

It has been shown earlier, that there is a good texture discrimination between tumour and healthy brain tissue. The discrimination analysis was carried out using the first and the second order statistics in which they are automatically chosen, so we calculate the brightness changes in pixels and between pixels. In this work the co occurrence matrix is set to calculate the changes in the gray level for five pixel distance (d = 5) and for four angles (0, 45, 90, and 135). This will give a large number of parameters for discrimination (as described in the introduction).

Apart from small variations, cancer cells are very much similar to the healthy cells; these variations are small and linked with certain substances such as cancer markers and other small biochemical changes which may have a little contribution in the image formation and disease recognition. If these changes are strong enough to give changes in the signal, it will change the pixel values and eventually the gray level distribution which can be detected by computer. Other factors

which are more effective in MRI image such as blood supply and water content as well as the presence of necrotic cells.

It is well known that MRI image originated from the unpaired protons within the molecule and influenced by the molecular shape, size and energy and the signal is mainly came from hydrogen atom because it has unpaired proton and high gyro magnetic ratio (20), then regions with an increased hydrogen atoms give stronger signal meaning that the higher water content the higher the signal similarly the higher blood perfusion the higher the signal. This suggests that changes in the effective molecular constituent or quantity may influence our analysis. Small changes in gray level may not be detected by eye because the human eye can not recognise small changes in the gray level in addition to the small size of the pixels. However, texture analysis for these small changes may hide interesting features which can give certain characteristics indicates the tumour advancement and tumour regions as well as the oedema according their difference in the regional constituents.

Tissue thickness and the cells density forming the mass as well as the necrotic tissue can also influence the MRI image brightness. Tissue density is also influence the x-ray and CT scanner images but on a different principle.

It appears that the discrimination between tumour and healthy tissue using MaZda is highly significant when calculating (p) value, Tables (1, 2, 3 and 4). It is unfortunate that some times comparison between the same tissues for different people give different texture probably caused by slight natural differences between people (unpublished data) and to difference in MRI equipment behaviour. This will add more complication to establish general figures to distinguish between tumour and healthy tissue. For this reason discrimination between tissues for the same person give more accurate results. Nevertheless, for brain tissue the differences between different individuals do not appear effective to a large extent. A close look at Tables (2, 3, and 4), one can see the sum of average for the tumour are similar over several pixels, the same thing can be observed for healthy tissue Table (5).

References

[1] J. J. Gibson, the Perception of Visual Surfaces, American Journal of Psychology, Vol. 63, 1950, pp. 367-384

[2] CA, Harlow SA. Eisenbeis, The analysis of radiographic images. IEEE Trans Comput 1973; C22:678-689.

[3] L.R. Schad, S. Blüml and I. Zuna, MR tissue characterization of intracranial tumors by means of texture analysis. Magn. Reson. Imaging 11 (1993), pp. 889–896.

[4] R.A. Lerski, K. Straughan, L.R. Schad, D. Boyce, S. Blüml and I. Zuna, MR image texture analysis: An approach to tissue characterization. Magn. Reson. Imaging 11 (1993), pp. 873–887.

[5] N. Petrick, H. Chan, B. Sahiner and D. Wei, An adaptive density-weighted contrast enhancement filter for mammographic breast mass detection. IEEE Trans. Med. Imaging 15 (1996), pp. 59–67.

[6] O. Salvetti, G. Braccini, R. Evangelista and M. Freschi, An intelligent system for the diagnosis of complex images. Artif. Intel. Med. 8 (1996), pp. 167–185.

[7] J. Peiss, M. Verlande, W. Ameling and R.W. Günther, Classification of lung tumors on chest radiographs by fractal texture analysis. Invest. Radiol. 31 (1996), pp. 625–629.

[8] Levin book M. Levine, Vision in Man and Machine, McGraw-Hill, 1985

[9] A. Materka, M. Strzelecki, Texture Analysis Methods – A Review, COST B11 report, Brussels, June 1998.

[10] P. M. Szczypiński M. Strzelecki, A. Materka and A. Klepaczko, MaZda-A software package for image texture analysis, computer methods and programs in Biomedicine 94, 1, April 2009, pp. 66-76.

[11] M. Hajek, M. Dezortova, A. Materka and R. Lerski, Editors, Texture Analysis for Magnetic Resonance Imaging, Med4publishing, Prague (2006).

[12] R. Haralick, K. Shanmugam, I. Dinstein, Textural Features for Image Classification, IEEE Transactions on Systems, Man and Cybernetics, 3, 6, 1973, 610-621.

[13] R. Haralick, Statistical and Structural Approaches to Texture, Proceedings IEEE, 67, 5, 1979, 786-804.

[14] F. Argenti, L. Alparone and G. Benelli, "Fast Algorithms for Texture Analysis Using Co-Occurrence Matrices", IEE Proceedings, 137, F, 6, 1990, 443-448.

[15] S. Mallat, "Multifrequency Channel Decomposition of Images and Wavelet Models",IEEE Trans. Acoustic, Speech and Signal Processing, 37, 12, 1989, 2091-2110.

[16] A. Laine and J. Fan, "Texture Classification by Wavelet Packet Signatures", IEEE Trans. Pattern Analysis and Machine Intelligence, 15, 11, 1993, 1186-1191.

[17] A.Jain, Fundamentals of Digital Image Processing, Prentice Hall, Englewood Cliffs 1989.

[18] M. Strzelecki, P. Szczypiński, MaZda Texture Analysis Software Institute of Electronics,Technical University of Lodz, Poland COST B11 action (1998-2002), Quantitation of Magnetic Resonance Image Texture.

[19] A. R. Webb, Statistical Pattern Recognition, John Wiley & Sons,Ltd, 2004.

[20] S. Thomas, E. James, C. Robert, Christensen's, Introduction to the physics of diagnostic Radiology, Lea and Filiger, Philadelphia, 1984.

<div dir="rtl">

الخلاصة

اجري الأختبار التحليلي لبنية او لخصائص تركيبيه لأربعة صور مأخوذه بالرنين المغناطيسي ولاربعة مرضى ممن ثبتت اصابتهم بورم الدماغ (Brain tumor) بواسطة برنامج مازده (MaZda) والهدف من التحليل هو ايجاد فروق تميز بين النسيج الدماغي الصحيح ونسيج الورم المرادف لنفس النسيج ولكل مريض.

اخذت ثلاثة مناطق في الورم وثلاثة اخرى في النسيج الصحيح المرادف. اظهرت النتائج تمايز واضح بين النوعين من النسيج، واعطت معامل فشر (Fisher coefficient) بين (138.5 و 547.5) وقيمة صغيرة جدا للاحتمالية (p value) اقل من 0.01 بكثير، يعتقد ان هذا التمايز يعود بصورة رئيسية الى احتمالية وجود

</div>

<div dir="rtl">

الخلايا الميتة والى الكتلة الكثيفة من الخلايا المكونة للورم والتي من الممكن قد غيرت مقدار كمية الدم الواصلة الى الورم والذي يؤثر على اشارة الرنين المغناطيسي.

</div>